JCARME
ISSN: 2228-7922
Journal of Computational and Applied Research in Mechanical Engineering
Vol. 8, No. 2, pp. 177-187
jcarme.sru.ac.ir

Numerical investigation of vertical and horizontal baffle effects on liquid sloshing in a rectangular tank using an improved incompressible smoothed particle hydrodynamics method

R. Shamsoddini

Department of Mechanical Engineering, Sirjan University of Technology, Sirjan, 7813733385, Iran

Article info:

Received:	04/04/2017
Accepted:	06/08/2018
Online:	06/08/2018

Keywords:
Smoothed Particle Hydrodynamics (SPH),
Vertical baffle,
Horizontal baffle,
Free surface.

Abstract

Liquid sloshing is a common phenomenon in transporting liquid tanks. Liquid waves lead to fluctuating forces on the tank wall. If the fluctuations are not predicted or controlled, they can lead to large forces and momentum. Baffles can control liquid sloshing fluctuations. One numerical method, widely used to model the liquid sloshing phenomena, is Smoothed Particle Hydrodynamics (SPH). Because of its Lagrangian nature, SPH is suitable for simulating free surface flow. In the present study, a relatively accurate Incompressible SPH (ISPH) method is improved by kernel gradient correction tensors, particle shifting algorithms, turbulence viscosity calculations, and free surface particle detectors is applied for the free surface flow modeling. In comparison to the other SPH simulations and experimental data, the results show that the present algorithm is effective for simulating free surface problems. The present algorithm is applied to simulate liquid sloshing phenomena, while the aim of this study is the investigation of vertical and horizontal baffle effects on the control and damping of liquid sloshing. Results show that, baffle size has a major role in sloshing fluctuation damping for vertical baffles. For horizontal baffles, also including size, the baffle base position has a significant role in liquid sloshing fluctuation damping. When horizontal baffle is near the free surface, sloshing fluctuation-damping increases.

1. Introduction

The liquid motion in vessels and containers is called sloshing. In fact, the motion of structure is transmitted to the liquid, so it is categorized as fluid-structure interaction (FSI). Currently, the interaction between fluid and structure is one of the most important problems in some industries. Pumps, turbines, airplanes, and ships are examples of FSI problems. To investigate such problems, experimental and numerical methods are used. Eulerian and Lagrangian methods are numerical methods which are applied to simulate FSI problems. Eulerian methods are usually grid-based, so the motion of a solid body grid should be defined and imposed during any iterations. Lagrangian and meshfree methods, such as Smoothed Particle Hydrodynamics (SPH), also could model the FSI. SPH was introduced by Lucy [1], and Gingold and

* *Corresponding author*
email address: shamsoddini@sirjantech.ac.ir

Monaghan [2] in 1977. In 1982, Gingold and Monaghan [3] used this method to simulate a compressible and inviscid flow. In 1997, Morris et al. [4] used SPH to model incompressible flow, which was developed to model related problems.

Newtonian flow [5, 6], non-Newtonian flow [7, 8], free surface flow [9], two-phase flow [9, 10], mixing flow [11-14], and FSI problems [7, 15] are examples in which SPH have widely been used. Weakly compressible SPH (WCSPH) and ISPH are two well-known SPH methods. WCSPH uses a state equation to calculate the pressure, while the ISPH method solves the Poisson equation to determine the pressure.

In this study, an ISPH algorithm is introduced to model a one-way coupled FSI problem with free surface flow. The SPH encounters special problems: particle clustering, defects, and tensile instability. So, this method evolves from the advanced discretization style, shifting algorithms, turbulence modeling, and free surface particle detecting. The method had also been assessed with previous results, including an experimental test. Because of the Lagrangian and meshless method, SPH could easily model free surface flow. Doring et al. [16] presented the SPH method for different kinds of free surface flow. Violeau and Issa [17] examined different turbulence models for the SPH simulations of flows; in SPHysics development, Gomez-Gesteira et al. [18] presented a free-surface fluid solver. The above scientists [16-18] used WCSPH. However, it is undermined by non-physical fluctuations in the density field. ISPH treats the WCSPH method [19], but recent efforts have been resolved to reduce non-physical fluctuations [5, 7] while ISPH was selected for the present simulations.

One of the most important problems in free surface flow is liquid sloshing in the tanks, which is a known phenomenon in liquid transport tanks. Sloshing phenomena may create great force and momentum, so controlling the tank and its carrier may be difficult and unsafe in this sense. Hence, predicting and controlling them are essential to the liquid transport industries. There is extensive research in this field. Bass et al. [20] investigated a scale modeling of liquefied natural gas sloshing in ship tanks. Dodge and Kana [21] experimentally and theoretically investigated the sloshing of tank liquid with a flexible, inextensible bladder. Hou et al. [22] simulated liquid sloshing behavior in a 2-D rectangular tank using the ANSYS-FLUENT software. Godderidge et al. [23] modeled sloshing flow in a rectangular tank with the commercial CFD code. SPH is also a convenient method to model liquid sloshing. There is research on this with the SPH method [24-27], while ISPH is also effective. The present ISPH algorithm is improved by the kernel gradient correction and shifting particles algorithm, while the turbulence viscosity calculator was also developed. The accuracy of the present algorithm is examined, even though there arestill valuable studies on sloshing phenomena to be carried out; some aspects have not been investigated yet. One strategy to reduce sloshing fluctuation is the baffle mechanism. In our study, both vertical and horizontal baffles are examined. The baffle position and size are accurate parameters in sloshing control. The results show that baffle size and position are essential parameters for pressure fluctuation in liquid tanks.

In the following, the numerical procedure is explained in details in section 2. In section 3, first, the accuracy of the present algorithm is evaluated, then, it is applied and examined for simulating the sloshing phenomenon and then the effect of vertical and horizontal baffles are investigated.

2. Equations and units

SPH is based on an integral approximation:

$$f(r) = \int_{\Omega} f(r') W(r - r', h)\, dr', \tag{1}$$

where h is the smoothing length, W is the kernel function, r is the position vector, and r' is the sub-integral variable. The integral form is approximated by a summation on the discrete points:

$$f(r) = \sum_j \forall_j f_j W(r - r_j, h). \tag{2}$$

Different kernel functions have been introduced and examined. However, it has been shown that the fifth-order Wendland kernel function is accurate to model fluid flow [28]. It is used as follows:

$$W(r,h) = W_0 \times \begin{cases} \left(1-\frac{|r|}{h}\right)^4 \left(4\frac{|r|}{h}+1\right) & 0 \le \frac{|r|}{h} < 1 \\ 0 & \frac{|r|}{h} \ge 1 \end{cases}. \tag{3}$$

For two-dimensional problems, W_0 is $\frac{7}{\pi h^2}$.

The governing equations are momentum and pressure Poisson equations, as follows:

$$\frac{d\boldsymbol{V}}{dt} = (\nu+\nu_t)\nabla^2\boldsymbol{V} + \boldsymbol{g} - \frac{\nabla p}{\rho}, \tag{4}$$

$$\nabla.\left(\frac{1}{\rho}\nabla p^{n+1}\right)_i = \frac{\nabla.\boldsymbol{V}_i^{*,n+1}}{\Delta t}, \tag{5}$$

where ρ, $\boldsymbol{V}, p,$ and ν are the fluid's density, velocity, pressure, and viscosity, and where ν_t is the turbulent viscosity. Furthermore, g is the gravitational acceleration and $\boldsymbol{V}_i^{*,n+1}$ is the intermediate velocity.

This algorithm was developed to model special problems in which the effect of free surface and forced motion of solid boundaries are considered. To overcome SPH defects, some modifications are needed. The present algorithm contains the main body and different sub-algorithms, adjusted according to an ISPH algorithm by Shamsoddini et al. [12]. Other sub-algorithms added are:

1- Forced motion of structures
2- Free surface detectors
3- Turbulence viscosity calculators
4- Shifting algorithms

In the algorithm, a predictor-corrector scheme has been implemented as well. In the first step, according to the gravitational and viscous terms of momentum equations (e.g., the velocity is predicted as follows [4]:

$$\boldsymbol{V}_i^{*,n+1} = \boldsymbol{V}_i^n + \left(\boldsymbol{g} + \sum_j 2\forall_j(\nu+\nu_t)\frac{\boldsymbol{V}_i-\boldsymbol{V}_j}{r_{ij}}\boldsymbol{e}_{ij}.\left(\boldsymbol{B}_i.\nabla W_{ij}\right)\right)\Delta t, \tag{6}$$

where $\boldsymbol{e}_{ij}$ is the unit vector (from j-th particle to i-th particle), W is the kernel function, $\forall_j$ is the volume of j-th particle, and $\boldsymbol{B}$ is the kernel gradient corrective tensor, proposed by Bonet and Lok [29]:

$$\boldsymbol{B}_i = -\left[\sum_j \forall_j \boldsymbol{r}_{ij}\nabla W_{ij}\right]^{-1}. \tag{7}$$

Thus, ν_t is turbulent viscosity, calculated by:

$$\nu_t = (c_s\delta)^2\left|\bar{S}\right|, \tag{8}$$

where $c_s = 0.2$, δ is the particle spacing and $\left|\bar{S}\right| = \left(2S_{ij}S_{ij}\right)^{0.5}$ S is the strain rate of the mean flow [30, 31]. After calculation of intermediate velocity, pressure is calculated to Eq. (5):

$$\sum_j 2\frac{\forall_j}{\rho_{ij}}\frac{p_i^{n+1}-p_j^n}{r_{ij}}\boldsymbol{e}_{ij}.\left(\boldsymbol{B}_i.\nabla W_{ij}\right) = \frac{\left\langle\nabla.\boldsymbol{V}_i^{*,n+1}\right\rangle}{\Delta t}. \tag{9}$$

If i th particle is on the free surface, then pi is set to equal zero. To detect free surface particles, a sub-algorithm is developed. For each particle, $\nabla.\boldsymbol{r}$ is calculated. For the two-dimensional case, $\nabla.\boldsymbol{r} = 2.0$, SPH discretization of $\nabla.\boldsymbol{r}$ would be:

$$\left\langle\nabla.\boldsymbol{r}\right\rangle_i = \sum_j \forall_j\left(\boldsymbol{r}_j - \boldsymbol{r}_i\right).\nabla W_{ij}. \tag{10}$$

However, $\nabla.\boldsymbol{r}$ would be less than two for free surface particles; in addition, all particles with $\nabla.\boldsymbol{r} < 1.6$ can be seen as free surface particles. After calculating pressure, velocity is corrected below:

$$\boldsymbol{V}_i^{n+1} = \boldsymbol{V}_i^{*,n+1} - \left\langle\frac{\nabla p}{\rho}\right\rangle_i^{n+1}\Delta t. \tag{11}$$

Another sub-algorithm is the definition of force motion of solid bodies. In this section, the formulation of motion for solid particles shows special motion and is defined. For all particles, the new position is calculated:

$$\boldsymbol{r}_i^{n+1} = \boldsymbol{r}_i^n + \boldsymbol{V}_i^{n+1}\Delta t. \tag{12}$$

Defects, tensile instability, and clustering distributions are SPH modeling complications. A shifting algorithm was used by Shamsoddini et al. [11-13] to prevent them. First, $\Delta\boldsymbol{r}_i$ is calculated as the shifting particle vector:

$$\Delta\boldsymbol{r}_i = \varepsilon\overline{\boldsymbol{r}}_i, \tag{13}$$

where ε is a constant varying between 0 and 0.1 and $\overline{\boldsymbol{r}}$ is:

$$\overline{\boldsymbol{r}}_{\boldsymbol{i}} = \sum_j \forall_j \boldsymbol{r}_{ij} W_{ij}. \tag{14}$$

Homogeneous distribution of the particles around the particle i leads to $\overline{\boldsymbol{r}}_{\boldsymbol{i}}$ =0.0. If $\overline{\boldsymbol{r}}_{\boldsymbol{i}} \neq$0.0, then the particle is shifted by $\Delta\boldsymbol{r}_i$. Finally, it is necessary to correct the flow field variables in the new position. According to the first order Taylor series expansion, these corrections are:

$$\Delta\boldsymbol{V}_i = \Delta\boldsymbol{r}_i.\langle\nabla\boldsymbol{V}\rangle_i, \tag{15}$$

$$\Delta p_i = \rho_i \Delta\boldsymbol{r}_i.\left\langle\frac{\nabla p}{\rho}\right\rangle_i. \tag{16}$$

Near each wall boundary, two rows of dummy particles are arranged. The velocity of each dummy particle is calculated by its corresponding position. If the wall has linear motion or is fixed, the velocity of the dummy particle is the same as its corresponding wall particle. For rotational cases, the angular velocity of the dummy particles and wall particles are the same. The pressure equation for dummy particles is obtained by dot multiplying the normal vector of the surface (n_w) by the momentum equation:

$$\left(\frac{\nabla p}{\rho}\right).\boldsymbol{n}_w = \frac{1}{\rho}\frac{\partial p}{\partial n_w} = -\frac{d\boldsymbol{V}_{\boldsymbol{b}_i}}{dt}.\boldsymbol{n}_w + \nabla.\left(\nu_e \nabla\boldsymbol{V}\right).\boldsymbol{n}_w + \boldsymbol{g}.\boldsymbol{n}_w. \tag{17}$$

Because of the fixed position of dummy particles, relative to the wall particles, the above equation can be discretized according to the finite difference method:

$$p_i^{n+1} = p_i^n + \rho\delta_n \begin{pmatrix} -\dfrac{d\boldsymbol{V}_{\boldsymbol{b}_i}}{dt}.\boldsymbol{n}_w \\ +\nabla.\left(\nu_e\nabla\boldsymbol{V}\right).\boldsymbol{n}_w + \boldsymbol{g}.\boldsymbol{n}_w \end{pmatrix}_i^n, \tag{18}$$

where δ_n is the distance between dummy particles and corresponding wall particles. In many cases, the second term of the right-hand side of the equation is small and can be neglected. If wall velocity is constant, the equation is converted to Neumann conditions for pressure.

The algorithm applied in the present study enables us to model fluid flow with the free surface engaged in moving rigid bodies. In the next section, two problems for validation, as well as the proposed algorithm, are examined to determine accuracy.

3. Results and discussion

Before modeling, the present numerical method has been examined against experimental and numerical results already reported. The problem for validation of the present code is the collapse of a tank water column, due to gravity. This is a traditional problem to test codes developed for free surface flow. Present code is compared with experimental data and other particle method simulations. The liquid sloshing problem is defined and modeled, and strategies are considered to control the sloshing fluctuations which are examined and discussed.

3.1. Collapse of a tank water column

This problem is known as dam breaking, and its geometrical properties are shown in Fig. 1. Dam breaking is an interesting problem for the SPH modeling. One of the first SPH modelings of the dam breaking was done by Bonet and Lok [28]. Although they introduced and used a corrected SPH method according to kernel gradient correction, they used a WCSPH method, and it is showed that the ISPH method is more accurate [19]. Also, they didn't consider the turbulence effects.

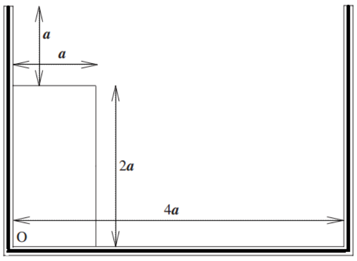

Fig. 1. The initial conditions of dam breaking problem.

Height of water column is twice its width. The gravity force causes the liquid to flow down and right. A continuous fluid flow is observed along the horizontal surface (Fig. 2(a)) until the liquid reaches the vertical wall. Then, the liquid goes up along the right-hand side vertical wall (Figs. 2(b) & 2(c)). After that, the liquid returns and is accumulated, as shown in Fig. 2(d). It is a common assumption that the 3D effects are neglected in the dam breaking problems modeling [17, 19, 29]. In Fig. 2, an agreement is seen between the present numerical simulations and those obtained experimentally by Doring et al. [16].

To examine this quantitatively, the results of the present code are compared with those obtained experimentally by Koshizuka and Oka [32] and numerically by Violeau and Issa [17], as seen in Fig. 3. In this figure, the non-dimensional position of the flow's leading edge, versus non-dimensional time, is plotted. As shown, the results of this study are closer to the experimental results than those obtained by the SPH k-ε method reported by Violeau and Issa [17]. However, there is a considerable difference between the laminar case and the experimental data. It shows obviously the effect of considering turbulence and Sub_Particle scale. Given the results of the present simulation in comparison with the experimental data, it seems that the present algorithm can be used to model free surface problems. It can also be applied to the model liquid sloshing problem.

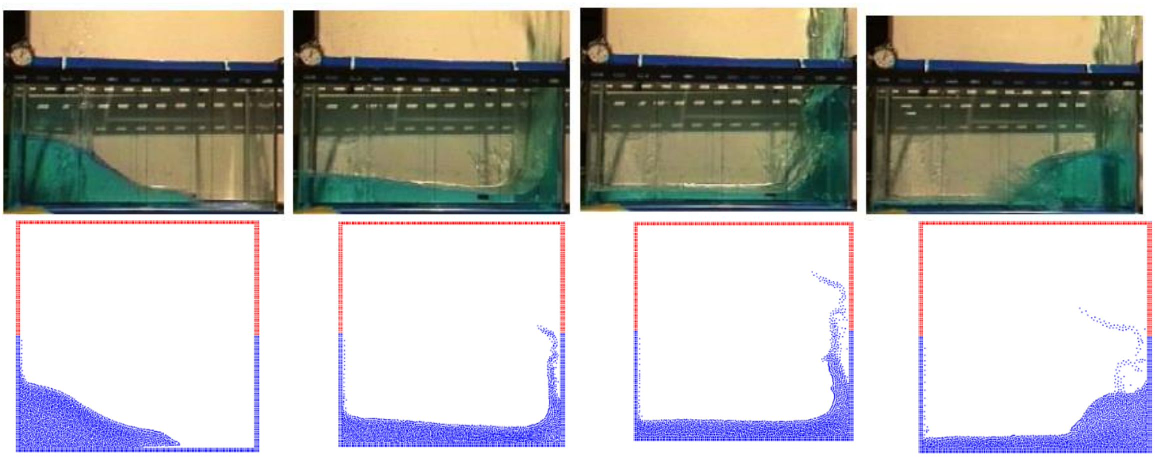

(a) (b) (c) (d)

Fig. 2. Qualitative comparison between experimental data (above row) and present SPH method (bottom row).

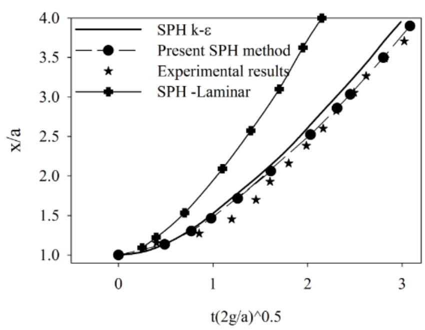

Fig. 3. Comparison among the present results, SPH k-ε [17], experimental results [23], and laminar SPH modeling (SPH without Sub_Particle scale) for the non-dimensional position of leading edge of flow.

3.2. Sloshing modeling

As mentioned, liquid sloshing is a challenging problem. In this phenomenon, the unwanted forces and fluctuations may create greater forces and momentum, which must be estimated. If these effects are not controlled or predicted, they may cause more problems in the liquid transportation system. Controlling and damping the fluctuation domain is the aim of the present work, as stated. Before this, it is necessary to predict the fluctuation domain and order of forces created in the tank. The free surface flow and fluctuations due to external sinusoidal excitation are investigated, and strategies to reduce them are examined. The initial conditions and geometrical properties of the sloshing problem are shown in Fig 4.

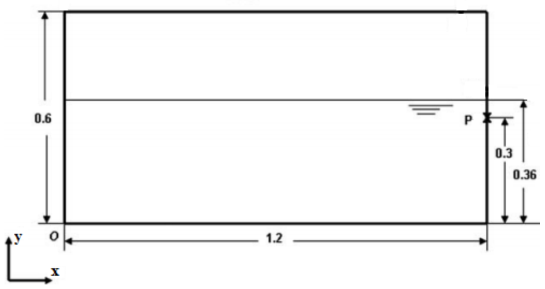

Fig.4. The geometrical and initial conditions of the sloshing problem.

After investigation of the particles resolution, the results of the present SPH modeling are compared with the previous cases. The same physical and geometrical tank model are selected as that previously examined by Godderidge et al. [23]. The tank motion is defined as:

$$x = A\sin\left(\frac{2\pi t}{T}\right), \qquad (19)$$

where A = 0.015m and T = 1.404s. They used a mesh-based two-phase method to model the sloshing phenomena. It is interesting to compare the results of the present particle method with their own. Fig. 5 illustrates the variation plot of free surface at t = 6.08T for both present simulations as seen in the results reported by Godderidge et al. [23]. It showsa strong agreement between the two numerical methods. Because of the neighboring particles search, the SPH method is categorized into the slow numerical methods. For the present simulation, the central processing unit (CPU) time per simulated second is about 4.12 h/s. However, the CPU time for mesh-based finite volume method (FVM) is about 1.42h/s for the homogeneous model and about 3.54 h/s for the inhomogeneous model [23]. The difference between the CPU time per simulated second for the inhomogeneous model and the SPH simulation is about 16%. It is expected that the SPH simulation is a more time-consuming process in comparison with the FVM method. In the SPH modeling, the second phase (air) is neglected by exerting the zero pressure condition on the free surface particles. So, the domain of solution for the SPH modeling becomes smaller than that for the mesh based two-phase modelings.

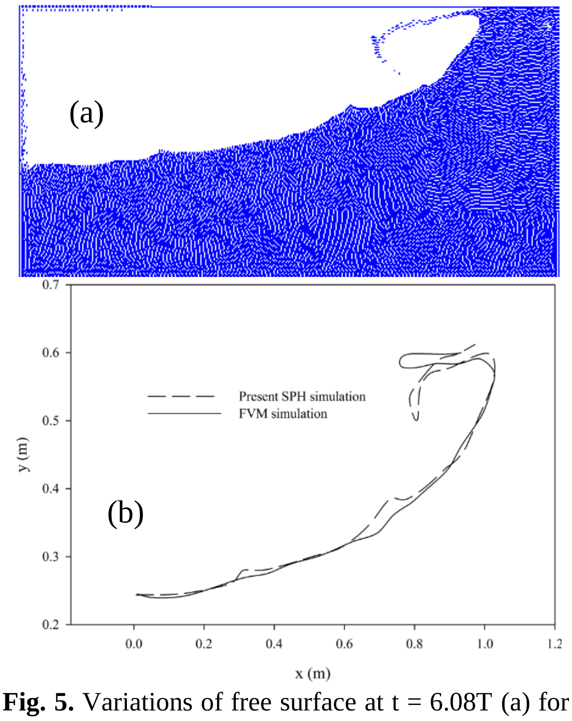

Fig. 5. Variations of free surface at t = 6.08T (a) for the present simulation and it in comparison with FVM results (b) reported by Godderidge et al. [23].

The pressure time history of a fixed point on the height of H/L=0.5, from the bottom of the tank vs. the experimental results of Hinatsu [33] is also shown in Fig. 6. It should be mentioned that the experimental data in Fig. 6, along with its plot, is obtained by conducting Fourier decomposition on the results of Hinatsu [33], as reported by Godderidge et al. [23]. As shown in this figure, a strong agreement is present between present results and those found experimentally. The results of Fig. 6 show that the pressure variation is a periodic function of time.

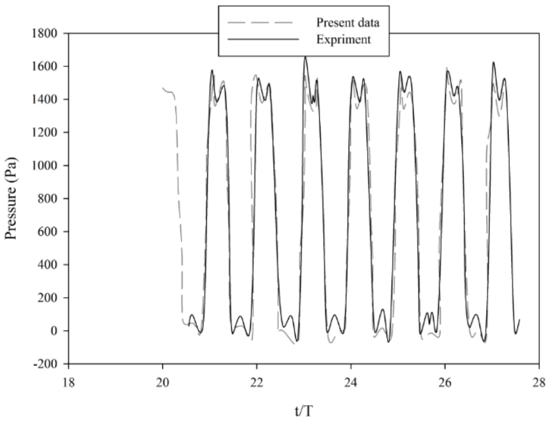

Fig. 6. Pressure time history of a fixed point of height h/L = 0.5 from the bottom of the tank, compared to the experimental results of Hinatsu [33].

The force sinusoidal motion of the tank is gradually transmitted to the fluid. A periodic flow is also created in the tank. The periodic flow can be detected by following the contours in Fig. 7.

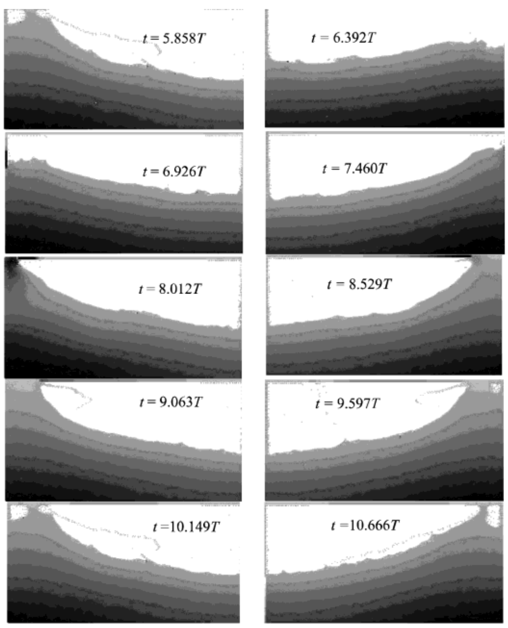

Fig. 7. Liquid motion and variations of free surface at different time periods involve motion.

In this figure, the contour of pressure variation and particle position are shown. The fluid particles continuously move up and down along the vertical walls of the tank. This leads to periodic pressure variation. If the motion of fluid particles along the vertical walls is limited, pressure variation is also reduced. Use of vertical baffles is a useful strategy to control fluctuations. The vertical baffle effect on fluctuation reduction is examined in the next subsection.

3.3. Vertical baffles

As mentioned, one important way to control the fluctuations is through baffles; they reduce the kinetic energy of fluid particles, thus, reduce the fluctuation domain. In Fig.8, contours of pressure and particle distribution of a tank with a vertical baffle are shown. In this case, the size of the baffle is half the size of the vertical walls of the tank. As shown in Fig. 8, the fluid motion along the vertical walls is restricted in comparison to that of Fig. 7.

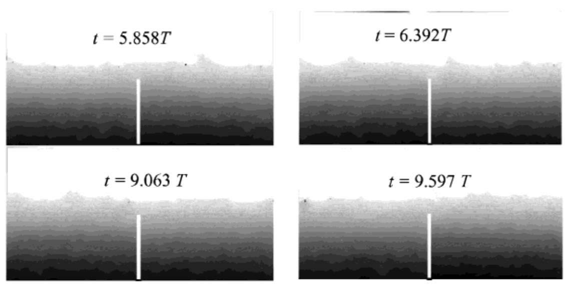

Fig. 8. Liquid motion and free surface variation at different times in the presence of vertical baffle.

The baffle size has a special effect on fluctuation damping. Reducing the fluctuation domain size is shown in Fig. 9. By increasing the baffle size, the fluctuation domain is reduced. The results show that by selecting a proper vertical baffle, fluctuations in a tank can be well-controlled. However, it may be that horizontal baffles also dampen the fluctuations as well as the vertical baffles. The effect of horizontal baffles on the fluid flow in a tank, due to sinusoidal motion, is discussed in the next subsection.

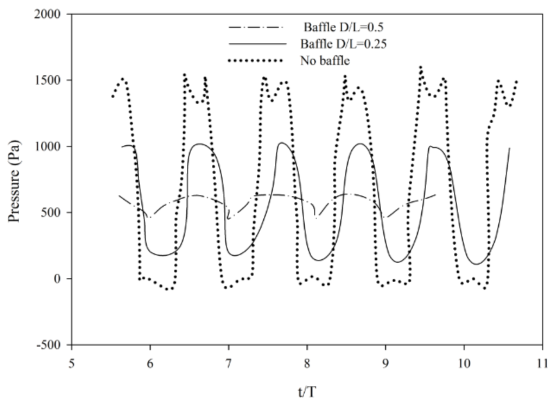

Fig. 9. The baffle size effect on pressure variation of a fixed point on the right wall at height H/L = 0.5.

3.4. Horizontal baffles

The horizontal baffles seem to be another useful method to control the fluctuations. Two horizontal baffles are considered for each vertical wall. For the first investigation, the size of baffles is considered as D/L = 0.5, while the height of the base of the baffle from the bottom wall is h_b $/L$= 0.6. All other physical and geometrical conditions are the same as the two previous cases. This is due to force sinusoidal motion as shown in Fig. 10.

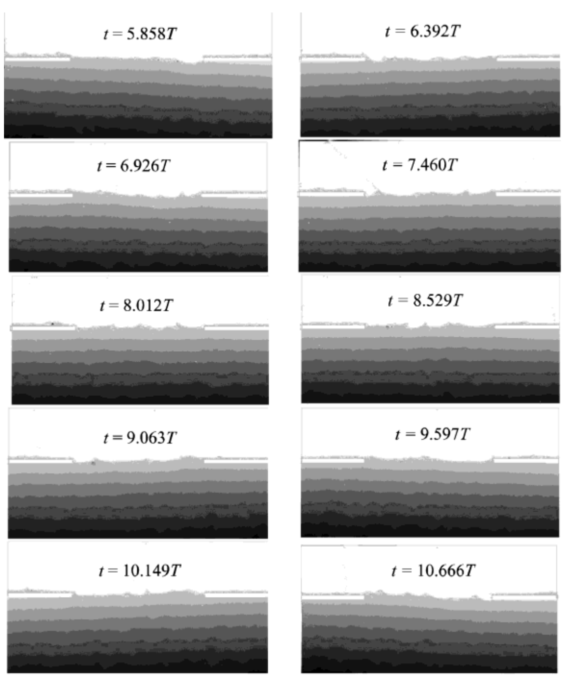

Fig. 10. Liquid motion and variation of the free surface at different time periods in the presence of horizontal baffles.

The fluctuation domain is controlled by the horizontal baffles. The size effect of the baffle on fluctuation damping is shown in Fig. 11.

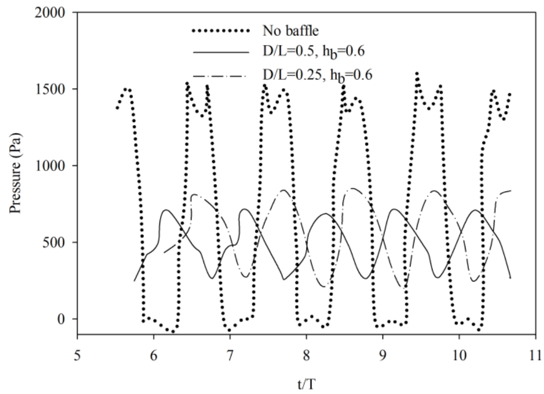

Fig. 11. The size effect of the baffle, which is tangential to the free surface at the initial time (h_b/L = 0.6) on pressure variation at a fixed point on the right wall at height H/L = 0.5.

Here, the pressure time variation of a point at the height H/L = 0.5 is plotted for three cases. The first case has no baffle, while the second and third cases have baffles with D/L = 0.25 and D/L = 0.5, respectively. As indicated for both baffle cases, the fluctuation domain is reduced considerably. However, it seems that the size for horizontal baffles is not as effective as that for vertical baffles. In this case, the baffles are set in such a way that they are tangential to the free surface of the liquid. The vertical motion of the fluid particles is restricted initially. It is critical to understand the effect of baffle position on flow and fluctuation. The position of the baffle base is decreased to h_b/L = 0.3. For this case, the pressure variation for the point on the height H/L = 0.5 for two baffles with different sizes (D/L = 0.25 and D/L = 0.5) and the case without a baffle is plotted in Fig. 12 for better comparison. For the case of D/L = 0.25, the fluctuations are close to those without a baffle. However, increasing the baffle size decreases the fluctuations. There are considerable differences between the plots of Fig. 11 and Fig. 12. First, decreasing the position of the baffle base causes an increase in the fluctuation domain. Second, in opposition to the case with h_b/L = 0.6, for the case with h_b/L = 0.3, baffle size has an effect on fluctuation damping.

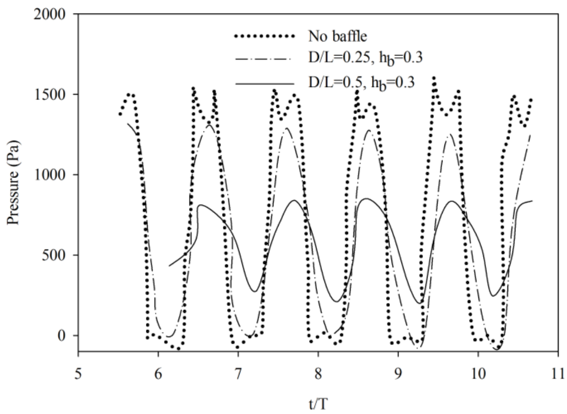

Fig. 12. The size effect of the baffle on the pressure variation at a fixed point on the right wall at height H/L = 0.5 for the case with $h_b/L=0.3$.

4. Conclusions

In the present study, a relatively accurate SPH method is applied to model the liquid sloshing phenomena. The SPH algorithm for solving the pressure Poisson and momentum equations contains various sub-algorithms, such as the kernel gradient correction, shifting particle algorithms, turbulence viscosity calculators, and free surface detectors. The accuracy of the present algorithm is evaluated against the experimental and numerical methods. The comparing results show that the applied algorithm is a proper method to model the free surface flow. It is also applied to model the liquid sloshing phenomena. To control them, vertical and horizontal baffles are examined and show that baffle size has a major role in sloshing fluctuation damping. For baffle size with D/L = 0.5, the fluctuation domains are damped considerably, and are reduced more than 85% in comparison with the case without any baffling. When the baffle size is reduced to D/L = 0.25, the fluctuation reduction is approximately 40%. The other case investigated is horizontal baffle. Baffle base position is more important than its size. When the baffle is tangential to the initial free surface (h_b /L= 0.6), the most efficient case is observed. For this, baffle size had less effect on the fluctuation reduction than other cases. By decreasing baffle base position (h_b/L = 0.3), the fluctuation reduction decreases as well, due to baffles. In this case, the baffle size should also be important.

References

[1] L. B. Lucy, “A numerical Approach to the Testing of the Fission Hypothesis”, *The Astronomical Journal*, Vol. 82, pp. 1013-1024, (1998).

[2] R. A. Gingold, and J. J. Monaghan, “Smoothed Particle Hydrodynamics: Theory and Application to Non-spherical Stars”, *Monthly Notices of the Royal Astronomical Society*, Vol. 181, pp. 375-389, (1997).

[3] R. A. Gingold, and J. J. Monaghan, “Kernel estimates as a basis for general particle methods in hydrodynamics,” *Journal of Computational Physics*, Vol.46, No. 3, pp. 429-453, (1982).

[4] J. P. Morris, P. J. Fox, and Y. Zhu, “Modeling low Reynolds number incompressible flows using SPH”, *Journal of Computational Physics*, Vol. 136, No. 1, pp. 214-226, (1997).

[5] M. Sefid, R. Fatehi, and R. Shamsoddini, “A modified smoothed particle hydrodynamics scheme to model the stationary and moving boundary problems for Newtonian fluid flows,” *Journal of Fluids Engineering*, Vol. 137, No. 3, pp. 031201-9, (2015).

[6] M. S. Shadloo, A. Zainali, S. H. Sadek, and M. Yildiz, “Improved incompressible smoothed particle hydrodynamics method for simulating flow around bluff bodies”, *Computer Methods in Applied Mechanics and Engineering*, Vol. 200, No. 9-12, pp. 1008-1020, (2011).

[7] M. R. Hashemi, R. Fatehi, and M. T. Manzari, “SPH simulation of interacting solid bodies suspended in a shear flow of an Oldroyd-B fluid,” *Journal of Non-Newtonian Fluid Mechanics*, Vol. 166, No. (21-22), pp. 239-1252. (2011).

[8] R. Shamsoddini, N Aminizadeh, and M Sefid, “An improved WCSPH method to simulate the non-Newtonian Power-Law Fluid Flow Induced by motion of a Square Cylinder”, *Computer Modeling in Engineering & Sciences*, Vol. 105, No. 3, pp. 209-230, (2015).

[9] A. Farrokhpanah, B. Samareh, and J. Mostaghimi, "Applying Contact Angle to a Two-Dimensional Multiphase Smoothed Particle Hydrodynamics Model", *Journal of Fluids Engineering*, Vol. 137, No. 4, pp. 041303-12, (2015).

[10] M. S. Shadloo, A. Zainali, and M. Yildiz, "Simulation of single mode Rayleigh–Taylor instability by SPH method", *Computational Mechanics*, Vol. 51, No. 5, pp. 699-715. (2013).

[11] R. Shamsoddini, M. Sefid, and R. Fatehi, "Lagrangian simulation and analysis of the micromixing phenomena in a cylindrical paddle mixer using a modified Weakly Compressible Smoothed Particle Hydrodynamics Method", *Asia-Pacific Journal of Chemical Engineering*, Vol. 10, No. 1, pp. 112-122, (2015).

[12] R. Shamsoddini, M. Sefid, and R. Fatehi, "ISPH modelling and analysis of fluid mixing in a microchannel with an oscillating or a rotating stirrer", *Engineering Applications of Computational Fluid Mechanics*, Vol. 8, No. 2, pp. 289-298, (2014).

[13] R. Shamsoddini, and M. Sefid, "Lagrangian simulation and analysis of the power-law fluid mixing in the two-blade circular mixers using a modified WCSPH method," *Polish Journal of Chemical Technology*, Vol. 17, No. 2, pp. 1-10, (2015).

[14] R. Shamsoddini, M. Sefid, R. Fatehi, "Incompressible SPH modeling and analysis of non-Newtonian power-law fluids, mixing in a microchannel with an oscillating stirrer", *Journal of Mechanical Science and Technology*, Vol. 30, No. 1, pp. 307-316, (2016).

[15] M.R. Hashemi, R. Fatehi, and M.T. Manzari, "A modified SPH method for simulating motion of rigid bodies in Newtonian fluid flows", *International Journal of Non-Linear Mechanics*, Vol. 47, No. 6, pp. 626-638, (2012).

[16] M. Doring, Y. Andrillon, B. Alessandrini, and P. Ferrant, 2003, "SPH Free Surface Flow Simulation," *18th International Workshop on Water Waves and Floating Bodies*, At Le Croisic, France, (2003).

[17] D. Violeau, and R. Issa, "Numerical modelling of complex turbulent free-surface flows with the SPH method: an overview", *International Journal for Numerical Methods in Fluids*, Vol. 53, No. 2, pp. 277-304. (2007).

[18] M. Gomez-Gesteira, B.D. Rogers, A. J. C. Crespo, R.A., Dalrymple, M. Narayanaswamy, and J. M. Dominguez, "SPHysics - development of a free-surface fluid solver- Part 1: Theory and Formulations", *Computers & Geosciences*, Vol. 48, pp. 289-299, (2012).

[19] E. S. Lee, C. Moulinec, R. Xu, D. Violeau, D. Laurence, and P. Stansby, "Comparisons of Weakly Compressible and Truly Incompressible Algorithms for the SPH Mesh Free Particle Method", *Journal of Computational Physics*. Vol. 227, No. 18, pp. 8417-8436, (2008).

[20] R. L. Bass, E. B. Bowles, R. W. Trudell, J. Navickas, J. C. Peck, N. Yoshimura, S. Endo, and B. F. M. Pots, "Modeling Criteria for Scaled LNG Sloshing Experiments", *Journal of Fluids Engineering*, Vol. 107, No. 2, pp. 272-280, (1985).

[21] F. T. Dodge, and D. D. Kana, "Dynamics of Liquid Sloshing in Upright and Inverted Bladdered Tanks", *Journal of Fluids Engineering*, Vol. 109, No. 1, pp. 58-63, (1987).

[22] L. Hou, F. Li, and C. Wu, "A Numerical Study of Liquid Sloshing in a Two-dimensional Tank under External Excitations", *Journal of Marine Science and Application*, Vol. 11, pp. 305-310, (2012).

[23] B. Godderidge, S. Turnock, M. Tan, and C. Earl, "An investigation of multiphase CFD modelling of a lateral sloshing tank", *Computers & Fluids*, Vol. 38, No. 2, pp.183-193, (2009).

[24] X. Y. Cao, F. R. Ming, and A. M. Zhang, "Sloshing in a rectangular tank

based on SPH simulation", *Applied Ocean Research*, Vol. 47, pp. 241-254, (2014).

[25] H. Gotoh, A. Khayyer, T. Ikari, H. Arikawa, and K. Shimosako, "On enhancement of Incompressible SPH method for simulation of violent sloshing flows", *Applied Ocean Research*, Vol. 46, pp. 104-115, (2014).

[26] S. De Chowdhury, and S. A. Sannasiraj, "Numerical simulation of 2D sloshing waves using SPH with diffusive terms", *Applied Ocean Research*, Vol. 47, pp. 219-240, (2014).

[27] J. R. Shao, H. Q. Li, G. R. Liu, and M. B. Liu, "An improved SPH method for modeling liquid sloshing dynamics", *Computers & Structures*, Vol. 100-101, pp. 18-26, (2012).

[28] W. Dehnen, and H. Aly, "Improving Convergence in Smoothed Particle Hydrodynamics Simulations without Pairing Instability", *Monthly Notices of the Royal Astronomical Society*, Vol. 425 (2), pp. 1068-1082, (2012).

[29] J. Bonet, and T. S. Lok, "Variational and momentum preservation aspects of Smooth Particle Hydrodynamic formulation", *Computer Methods in Applied Mechanics and Engineering* Vol. 180, pp. 97-115, (1999).

[30] A. M. Aly, and S. W. Lee, "Numerical simulations of impact flows with incompressible smoothed particle hydrodynamics", *Journal of Mechanical Science and Technology*, Vol. 28, No. 6, pp. 2179-2188, (2014).

[31] R. Shamsoddini and N. Aminizadeh, "Incompressible Smoothed Particle Hydrodynamics Modeling and Investigation of Fluid Mixing in a Rectangular Stirred Tank with Free Surface", *Chemical Engineering Communications*, Vol. 204, No. 5, pp. 563-572, (2017).

[32] S. Koshizuka, and Y. Oka, "Moving-particle semi-implicit method for fragmentation of compressible fluid", *Nuclear Science Engineering*, Vol. 123, pp. 421-434, (1996).

[33] M. Hinatsu, "Experiments of two-phase flows for the joint research," Proceedings of the SRI-TUHH mini-workshop on numerical simulation of two-phase flows, *National Maritime Research Institute & Technische Universität Hamburg–Harburg, NMRI; (2001).*

How to cite this paper:

R. Shamsoddini, "Numerical investigation of vertical and horizontal baffle effects on liquid sloshing in a rectangular tank using an improved incompressible smoothed particle hydrodynamics method" *Journal of Computational and Applied Research in Mechanical Engineering*, Vol. 8, No. 2, pp. 177-187, (2018).

DOI: 10.22061/jcarme.2019.2437.1231

URL: http://jcarme.sru.ac.ir/?_action=showPDF&article=992